In-situ positron emission of CO oxidation

In-situ Positron Emission of CO Oxidation

K. A. Vonkeman, G. Jonkers, and S. W. A. van der Wal

Koninklijke/Shell-Laboratorium, Amsterdam (Shell Research BV), P. O. Box 3003, 1003 AA Amsterdam, The Netherlands

R. A. van Santen

Schuit Institute of Catalysis Laboratory of Inorganic Chemistry and Catalysis, Eindhoven, University of Technology, The Netherlands

Catalysis / Chemical Kinetics / Elementary Reactions / Isotopes / Metals

Using a Neuro ECAT positron tomograph the Positron Emission computed Tomography (PET) has been utilized to image the catalytic oxidation of CO by using CO and CO_2, labelled with short lived positron emitting nuclides. Studies were performed over highly dispersed ceria/γ-alumina supported platinum and rhodium catalysts. With a mathematical model of the reaction kinetics, based on the elementary steps of the catalytic reaction and partially on literature surface science data, the effect of CeO_2 promotion and the presence of NO were quantified in terms of the number of adsorption sites and adsorption equilibrium constants. Oxygen atoms of CO_2 remain much longer in the catalyst bed than the carbon atoms, which is due to carbonate formation at the Ceria surface and exchange of the oxygen atoms of these carbonate groups with the ceria lattice oxygen atoms. The heat of desorption of CO from the noble metal surface at low temperatures was found to be increased due to the presence of NO molecules at the surface. At higher temperatures NO dissociates, the adsorbed N and O atoms have a repulsive interaction with adsorbed CO molecules.

Introduction

Positron Emission Computed Tomography (PET) is a relatively new 3D imaging Technique emerging from nuclear medicine and is capable of mapping quantitatively the concentration of a positron emitting tracer [1,2]. In this paper its utilisation to study catalyst kinetics is described. One uses the labelling of reactants with positron emitting nuclides. We applied ^{11}C, ^{13}N and ^{15}O labelled molecules to study the oxidation of CO and reduction of NO by CO. Reactions of interest to automotive exhaust catalysis. The positron emission technique enabled to perform in-situ transient experiments. Once reaction was in its steady state a pulse containing an extremely small concentration of radiochemically labelled molecules was injected. Concentrations used were such that the overall reaction could be considered undisturbed. The time dependence of the radiochemical signal was followed through the reactorbed operated in plug flow.

Fig. 1 shows a schematic representation of the equipment in which the radioisotope experiments were carried out. The Neuro ECAT positron emission tomograph contains eight banks with each eleven BGO (Bismuth Germanate Oxide) detectors. These eight banks are placed in an octagonal arrangement, so that in imaging experiments a circular field of detection with a diameter of 21 cm is obtained.

For studying the kinetics of CO conversion processes a time resolution of the order of seconds is required. Using a injection monitor [4], a minimum temporal resolution of 1.2 s could be obtained with a spatial resolution of ±8 mm full width at half maximum [5]. To achieve this, coincidences of the γ-photons generated by annihilation of positron-electron pairs were measured between two detectors that view a single point on the reaction tube axis. In addition two 3-inch scintillation detectors were used: one facing the inlet tube and the other facing the outlet tube. The data registered by the tomograph are converted and stored. They data registered by the two opposing banks parallel to the reader tube can be used to construct a 1D image with 21 picture elements along the horizontal axis of the reactor tube.

By repeating the generation of these 1D images every 1.2 s a 2D (x,t) array is constructed. Resulting "reaction images" are presented throughout this paper.

The product gases exiting the reactor were analysed using a gaschromatograph and a Mass Spectrometer measuring the chemical conversions and a Radio Gas Chromatograph for measuring the distribution of the label over the different molecules.

To simulate the catalytic reaction use was made of a mathematical model, that enabled to compute overall kinetics on the basis of elementary reactionrate constants. A second order central discretisation method has been used for the numerical solution of the resulting coupled equations, as well as a moving grid approximation based on the method of lines [6].

The main ingredients of most commercial automotive exhaust catalysts are platinum, palladium, rhodium and ceria [7–13].

Here we report studies on CO oxidation catalysed by highly dispersed, ceria/γ-alumina supported platinum and rhodium catalysts in the presence and absence of NO.

The conditions have been chosen such that reactions are kinetically controlled. This implies the use of high linear velocities, small catalyst particles and low temperatures. Under those conditions noble metal surfaces are covered

  0005-9021/93/0303-00333 $ 10.00+.25/0

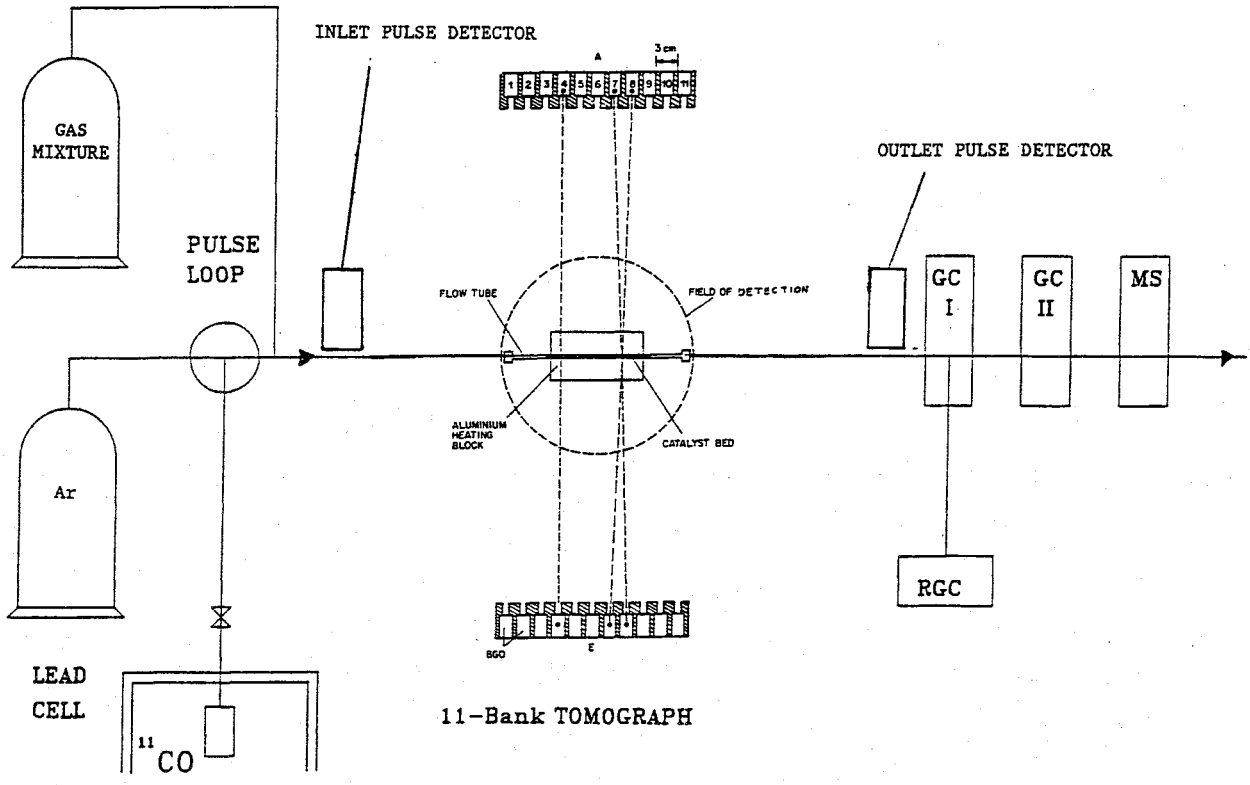

Fig. 1
A schematic drawing of the experimental set-up. The carrier gas (argon) is led through the pulse loop, where the labelled compound is taken up in the gas flow. The carrier gas is thereafter mixed with the reacting compounds and led over the catalyst bed in the reactor. The reactor tube is placed in the aluminium oven block, which is fixed exactly horizontal in the centre of the field of detection of the tomograph. At the reactor exit the product stream is analyzed making use of (radio) gas chromatography and mass spectrometry

for a high fraction by CO and rate-limiting to CO oxidation is the generation of free surface sites on which O_2 can dissociatively adsorb. At low temperatures very low concentrations of NO have been reported to inhibit CO oxidation by O_2 [20].

Cerium oxide, present in relatively high concentrations at the catalyst surface, has been ascribed a number of different functions in the catalyst [13,21]. Most studies on ceria promotion concentrate on the capacity of ceria to store oxygen, possible because Ce can exist in different valence states [11–26]. Ceria has also been found to promote CO oxidation [13,27,28] and the watergas shift reaction [13].

Experimental

Catalyst

The catalysts were prepared on an alumina carrier (ex Kaiser, Boehmite, Versal 250 Forming Grade) on which Ce $(NO_3)_3$, $6H_2O$ (ex Fluka AG, pro analyse) was impregnated to a concentration of 0.6% w CeO_2 After drying and calcination at 500°C noble metals were deposited by impregnation. Using $PtCl_4$ (ex Drijfhout) a catalyst with 0.12% w Pt was prepared, Rh $(NO_3)_3$. $2H_2O$ (ex Johnson Matthey) was impregnated to a concentration of 500 ppm. The catalysts were dried at 120°C and calcined at 500°C for one hour and then reduced for 2 hours at 300°C. Both catalysts had a porevolume of 0.60 ml/g and BET surface-area of 120 m/g. Other relevant catalyst characterization parameters are given in Tables 1.

Transient Experiments

Main features of the experiments are:

- Amounts of less than 0.1 nano moles of CO containing ca. 0.15 picomoles (or 50 mBq) of ^{11}CO or $^{11}CO_2$ in Argon, were extracted from a lead shielded container.
- These amounts were taken up into the gasmixture, which was continuously flowing through the catalyst bed in the reactor, without disturbing the pressure or the chemical composition of this gasflow (ca. 0.3 μmoles CO/s).
- The total gasflow of 40 ml/min STP, containing 1% CO, 0.5% O_2 and 10% CO_2 in argon was led over 3.9 g crushed catalyst, sieve fraction 30–80 mesh. Catalysts were submitted to a gasflow for at least 12 hours before starting the transient experiments.

The catalyst sample was placed in a 3/8 inch reactortube (Hoke stainless steel, internal diameter 7 mm, catalyst bed length 14 cm). Conditions were ambient pressure and $100°C < T < 170°C$. In a number of experiments 1400 ppm NO was added. 10% CO_2 was present in the gas mixture to bring CO_2 adsorption on CeO_2 to equilibrium.

Model of the Reaction Mechanism

We have used an adapted reaction mechanism, based on that proposed by Ertl [19] to model the kinetic experiments. The model contains three reaction steps for CO oxidation over noble metal surfaces and one for CO_2 interacting with the ceria:

CO adsorption to the noble metal surface (Me) (1)
CO desorption from the metal surface (−1)
irreversible dissociative O_2 adsorption at noble metal surfaces (2)
irreversible surface (CO/O conversion and CO_2 desorption) (3)
CO_2 adsorption to the carrier (CeO_2) (4)
CO_2 desorption from the carrier (−4)

The reactionrate constants (1), (2) and (4.1) can be deduced from the sticking probabilities. The desorption rate constants (−1) and (−4) and surface reaction rate constants (3)(are chosen to be of the Arrhenius form. As was reported by Yates et al. [29] and Oh et al. [30], the dissociative adsorption of oxygen is modelled best by using a first order dependence on the fraction of free surface sites.

Table 1a
Platinum catalyst characterization parameters used in the reaction model

Parameter	Value
Platinum dispersion	84%
Maximum CO/Pt ratio at platinum surface	1
CO adsorption capacity of Pt surface	$2.4 \cdot 10^{-5}$ mol/m^2
Total platinum surface in catalyst (3.9 g)	1 m^2
CO_2 adsorption capacity of CeO_2 at carrier	$5.6 \cdot 10^{-5}$ mol
CO_2 adsorption capacity of CeO_2 at Pt catalyst	$3.1 \cdot 10^{-5}$ mol

Table 1b
Rhodium catalyst characterization parameters used in the reaction model

Parameter	Value
Rhodium dispersion	100%
Maximum CO/Rh ratio at rhodium surface	1
CO adsorption capacity of Rh surface	$2.6 \cdot 10^{-5}$ mol/m^2
Total rhodium surface in catalyst (3.9 g)	0.5 m^2
CO_2 adsorption capacity of CeO_2 at carrier	$5.6 \cdot 10^{-5}$ mol
CO_2 adsorption capacity of CeO_2 at Pt catalyst	$5.8 \cdot 10^{-5}$ mol

Results and Discussion

CO Oxidation by O_2 Over Supported Platinum and Rhodium Catalysts

In Fig. 2, the results of four pulse experiments with the Pt/CeO_2 catalyst are shown. The data were simulated with the mathematical kinetic model to give the reaction parameters summarized in Tables 2.

In (2a) ^{11}CO was pulsed over SiC. Experiment 2B shows the time dependence of a $^{11}CO_2$ pulse. Product identification at the reactor exit indicated only $^{11}CO_2$. CO_2 strongly interacts with CeO_2 and little with Pt, hence from experiment 2B the rates of adsorption and desorption of CO_2 on Ceria could be obtained. Due to the relatively small temperature range in which the experiments were carried out (100°C−150°C), no activation energy for desorption could be obtained. Fig. 2c the reaction image of ^{11}CO, shows a residence time of the order of 100 s in the catalyst bed. This is due to the strong CO interaction with Pt. Little CO is converted because the platinum surface is completely covered by CO.

This experiment enabled determination of the rate constants of CO adsorption and desorption. The CO adsorption capacity found is 2×10^{-5} mol CO/m^2 Pt. Values used in simulation experiments (Table 2b) correspond well with literature values (31−33). The relatively high sticking coefficient of O_2 on the platinum surface is due to the promoting effect of the ceria present at the catalyst surface. The model proposed by Jin [27] in which O atoms are transferred from Ceria crystals to platinum crystals is supported by our experiments.

In Fig. 3, reaction images for Pt and Rh containing catalysts are compared. Temperatures were chosen such that CO and O_2 oygen conversion was 50% over both catalysts. A smoothing function was applied to the reaction images in Fig. 3 to improve signal to noise ratio. A comparison of Figs. 3b and 2d shows that the rhodium catalyst exhibits a stronger interaction with $^{11}CO_2$ than the platinum catalyst.

Table 2a
Kinetic reaction parameters used in the mathematical model

Reaction step		Parameter
1	S_{CO}	CO sticking probability at metal
−1	E_a/R	CO desorption activation energy
−1	k_0	CO desorption pre-exponential factor
2	S_{O_2}	O_2 sticking probability at metal
3	E_a/R	Reaction activation energy
3	k_0	Reaction pre-exponential factor
4	S_{CO_2}	CO_2 sticking probability at CeO_2
−4	k_{des}	CO_2 desorption from CeO_2 rate const.

Table 2b
Values used for kinetic reaction parameters for the platinum catalyst

Reaction step		Values used in this study	Values used by Lynch et al. (33)*)
1	S_{CO}	$8 \cdot 10^{-5}$	2×10^{-5}
−1	E_a/R	$9 \cdot 10^3$ K	$9 \cdot 10^3$ K
−1	k_0	$1.8 \cdot 10^{10}$ mol/m^3/s	$4 \cdot 10^9$ mol/m^3 s
2	S_{O_2}	$3.6 \cdot 10^{-7}$	$9 \cdot 10^{-9}$ $(= 150 \cdot 6 \cdot 10^{-11})$
3	E_a/R	$8 \cdot 10^3$ K	$8 \cdot 10^3$ K
3	k_0	$5.8 \cdot 10^{13}$ s^{-1} m^{-1}	$5.8 \cdot 10^{13}$ s^{-1} m^{-1}
4	S_{CO_2}	$6.6 \cdot 10^{-5}$	−*)
−4	k_{des}	7.9 s^{-1}	−*)

*) No ceria present in this catalyst.

Table 2c
Values used for kinetic reaction parameters for the rhodium catalyst

Reaction step		Values used in this study	Values as used by Oh et al. (20)*)
1	S_{CO}	$8 \cdot 10^{-5}$	(0.5)**)
−1	E_a/R	$1.3 \cdot 10^4$ K	$1.4 \cdot 10^4$ K
−1	k_0	$1.5 \cdot 10^{14}$ mol/m^3/s	$1.6 \cdot 10^{14}$ mol/m^3/s
2	S_{O_2}	$3.6 \cdot 10^{-7}$	(0.01)**)
3	E_a/R	$8 \cdot 10^3$ K	$7.2 \cdot 10^3$ K
3	k_0	$5.8 \cdot 10^{13}$ s^{-1} m^{-1}	$1 \cdot 10^{12}$ s^{-1} m^{-1}
4	S_{CO_2}	$1.2 \cdot 10^{-4}$	−*)
−4	k_{des}	7.9 s^{-1}	−*)

*) No ceria present in this catalyst.
**) Only the value for the initial sticking coefficients are given.

This indicates that a smaller area of the Ceria is covered by the active metal in the Rhodium catalyst than the Platinum catalyst. The shorter residence time of ^{11}CO on the Rhodium catalyst is due to two factors:

- The higher Rhodium surface area, than platinum (0.5 m^2 rhodium, versus 1 m^2 platinum)
- The higher CO desorption rate on the Rhodium catalysts, because of the higher temperature used (rhodium 150°C, versus platinum 130°C).

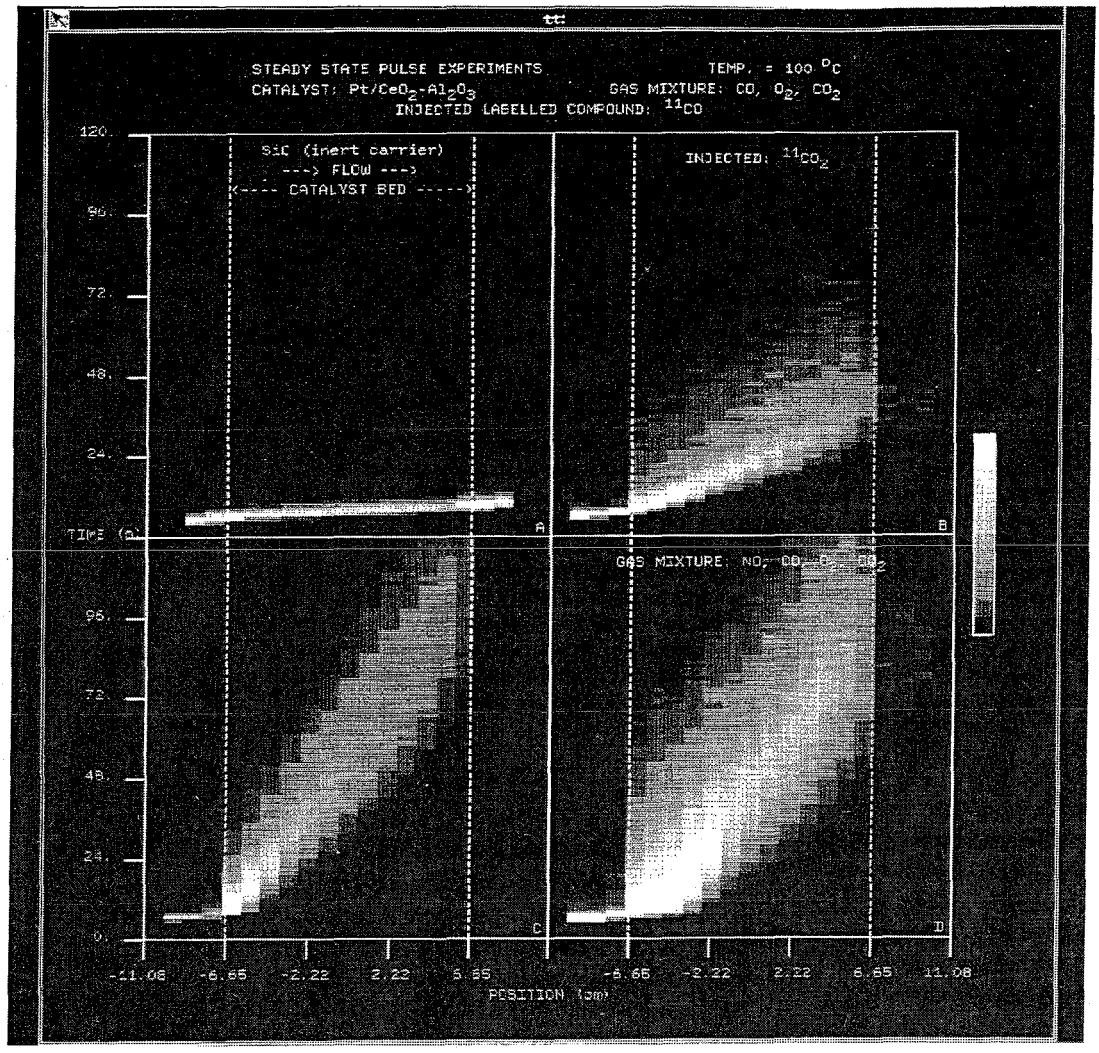

Fig. 2
The reaction images of four pulse experiments at 100°C. In the experiment shown in image A, an ^{11}CO pulse was led over an inert SiC bed. The reactor was continuously exposed to the standard gas flow, containing CO, O_2 and CO_2. The same reaction mixture was flowing through the reactor in the experiments shown in images B and C. Reaction image A shows the behaviour of inert gas molecules. In the other three experiments, the standard $Pt/CeO_2/\gamma\text{-}Al_2O_3$ catalyst was present in the reactor. In experiment B a pulse of $^{11}CO_2$ was given and in C and D pulses of ^{11}CO were injected. In experiment D also 1400 ppm NO was present in the gas flow

Values for elementary rate-constants used in the simulations are summarized in Tables 2. The most important difference between Pt and Rh for the CO oxidation reaction at low temperature is the higher desorption rate of CO from Rh compared to Pt.

The Influence of NO on the CO Oxidation by Supported Platinum

As NO exhibits a high sticking coefficients on platinum surfaces, the rate of adsorption of CO will become suppressed [18,34]. Fig. 2d shows an ^{11}CO pulse experiment over a platinum catalyst, which was exposed to the gasflow to which 1400 ppm NO was added.

Clearly a decrease in CO adsorption is observed. However, comparison of Figs. 2c and 2d indicates also an increased mean residence time. From this observation one concludes that the rate of CO desorption from the platinum surface has been changed by the presence of NO. Simulation established that about 60% of the platinum surface was covered by adsorbed NO molecules.

At the low temperatures used (T = 100°C) NO was found not to dissociate and was found to enhance the activation energy for CO desorption by 8 kJ/mol. This may be related to a report by Raval e.a. [35] showing that NO adsorbed to palladium surfaces decreases the CO desorption rate. NO present at the catalyst surface drives CO in the linearly adsorbed position in which it is stabilized by a dipole-inducing interaction between NO_{ad} and CO_{ads}.

The Exchange of CO_2-Oxygen Atoms with Ceria Lattice Oxygen

In Fig. 4, the movement of labelled carbon or oxygen atoms is followed through the catalyst bed. Interesting differences between the residence time of C and O in the catalyst bed are found especially due to the interaction with CeO_2.

In Fig. 4b the reaction image of a ^{11}CO pulse experiment is given, while in Fig. 4e a pulse of $C^{15}O$ was applied. The

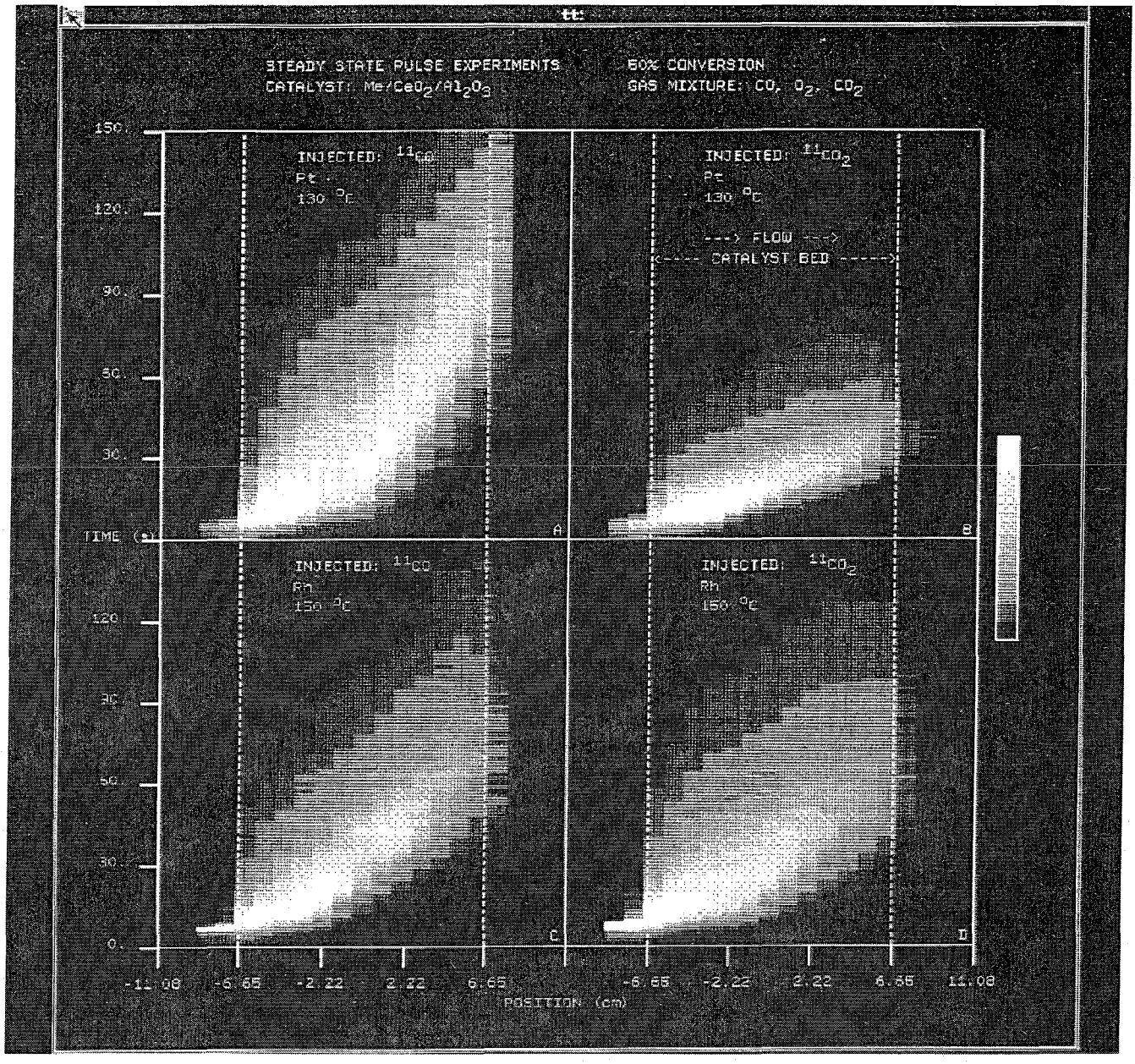

Fig. 3
The reaction images of four pulse experiments at which 50% conversion was reached. The standard gas mixture, without NO, was flowing through the catalyst bed in all four experiments. In experiments A and B the $Pt/CeO_2/\gamma\text{-}Al_2O_3$ catalyst was present in the reactor and the temperature was 130°C. In C and D the temperature was 150°C and the reactor was filled with the $Rh/CeO_2/\gamma\text{-}Al_2O_3$ catalyst. In A and C pulses of ^{11}CO were given while in B and D $^{11}CO_2$ was pulsed over the catalyst

oxygen atoms supplied with the CO molecules remain much longer in the catalyst bed than the carbon atoms of these molecules.

Similar observations are made for the labelled CO_2 molecules shown in Fig. 4c (a $^{11}CO_2$ pulse) and Fig. 4f (a $C^{15}OO$ pulse). One concludes that adsorbed CO_2 molecules dissociate at the Ceria surface and associate again before desorption. Upon adsorption of CO_2 carbonates are formed [28,36]. The scrambling of oxygen atoms of the carbonate groups and the ceria lattice leads to incorporation of 150 into the CeO_2 lattice giving long residence times. A probability of 1 to 7 or 8 for an oxygen atom to form a CO_2 molecule with the same carbon atom that adsorbed initially was established from these experiments.

The enhanced rate of O-exchange with CeO_2 lattice atoms [37] can probably be mediated by CO_2 formation. The O_2 molecules that dissociatively absorb on to the platinum surface, react with CO molecules and form CO_2, which desorbs from Pt. Readsorption of CO_2 leads to oxygen scrambling with lattice oxygen.

The reaction image 4d shows the result of an experiment using ^{15}OO, that can be explained by such a mechanism.

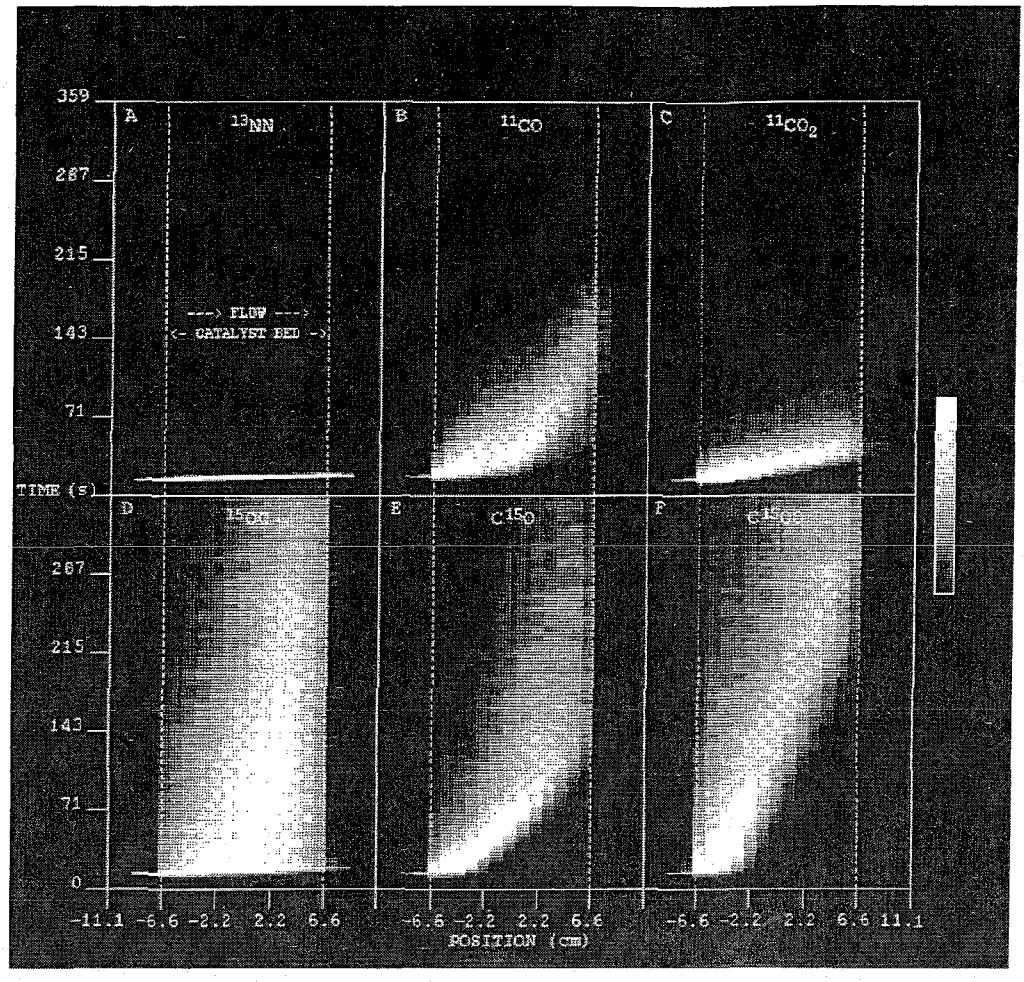

Fig. 4
A set of reaction images of pulse experiments over the $Pt/CeO_2/\gamma\text{-}Al_2O_3$ catalyst. Under identical conditions (standard gas mixture and flow rate, $T = 140°C$, 76% conversion), six different labelled compounds were pulsed over the catalyst. In experiment A ^{13}NN was pulsed over the catalyst, showing the behaviour of inert gas molecules. In B an ^{11}CO pulse experiment is shown, in C $^{11}CO_2$, in D ^{15}OO, in E $C^{15}O$ and in F $C^{15}OO$

Conclusion

Labelling of reactants with positron emitting nuclides gives useful information in studies of catalyst kinetics and reaction-mechanisms. Applied in transient kinetic experiments, surface coverages of reactants and intermediates at the catalyst surface under actual reaction conditions and reaction rates can be established.

The availability of information on the concentrations of reactants and intermediates at the catalyst surface increases the accuracy of the determination of the kinetic reaction parameters considerably. The extra information obtained with the positron emission technique results from the data obtained directly from the catalyst bed. Using positron emission tomography a reaction image can be constructed showing the concentration profile as a function of time and location.

The promoting effect of ceria in the CO oxidation by O_2 leads to an enhanced O_2 stickingscoefficient on Pt. At low temperatures the presence of NO blocks a significant fraction of the catalyst surface during reaction. The direct interaction with NO decreases the rate CO desorption.

A strong adsorption of CO_2 to CeO_2 was found, which probably leads to the formation of surface carbonate groups. Upon decompositon oxygen atoms from the carbonates exchange with the ceria surface.

References

[1] M. E. Phelps, J. C. Mazziotta, and H. R. Schelbert, Positron Emission computed Tomography and Autoradiography, Raven Press, New York 1986.
[2] S. Webb, Medical Science Series, The physics of medical imaging, Adam Hilger, Bristol 1980.
[3] Experiments have been carried out at the Institute for Nuclear Sciences at the State University of Gent, Belgium, see: Annual Report 1987, p. 99, Rijksuniversiteit Gent, Lab. for Analytical Chemistry, Ed. R. Dams, 1988.
[4] M. E. Phelps, E. J. Hoffmann, S. C. Huang, and D. E. Kuhl, J. Nucl. Med. *19* (6), 635 (1978).

[5] C. W. Williams, M. C. Crabtree, M. R. Burke, R. M. Keyser, S. G. Burgiss, E. J. Hoffman, and M. E. Phelps, IEEE Trans. Nucl. Sci. *NS-28*, 1736 (1981).
[6] J. G. Verwer, J. G. Blom, R. M. Furzeland, and P. A. Regeling: A moving grid method for a one-dimensional PDES based on the Methods of Line in J. E. Flaherty, P. J. Paslow, M. A. Schephard, J. D. Vaselakes: Adaptive methods for partial differential equations, *160* (1989).
[7] K. C. Taylor, in: Catalysis, Sience and Technology. J. R. Anderson, M. Boudart (eds.) *5* (2), 119 (1984).
[8] M. P. Walsh, Plat. Met. Rev. *30* (3), 106 (1986).
[9] J. T. Kummer, J. Phys. Chem. *90*, 4747 (1986).
[10] B. Engler, E. Koberstein, and P. Schubert, Appl. Catal. *48*, 71 (1989).
[11] H. C. Yao and Y. P. Y. Yao, J. Catal. *86*, 254 (1984).
[12] S. H. Ho and J. E. Carpenter, J. Catal. *98*, 178 (1986).
[13] B. Harrison, A. F. Diwell, and C. Hallett, Plas. Met. Rev. *32* (2), 73 (1988).
[14] M. R. Prairie, B. K. Cho, S. H. Oh, E. J. Shinonskis, and J. E. Bailey, Ind. Eng. Chem. Res. *27*, 1396 (1988).
[15] Y. E. Li, D. Boecker, and R. D. Gonzales, J. Catal. *110*, 319 (1988).
[16] H. Murali and Y. Fuyitani, Ind. Eng. Chem. Prod. Res. Dev. *25*, 414 (1986).
[17] S. E. Voltz, C. R. Morgan, D. Liederman, and S. M. Jacob, Ind. Eng. Class, Prod. Res. Dev. *12* (4), 294 (1973).
[18] G. B. Fischer, S. H. Oh, J. E. Carpenter, C. L. Dimaggio, S. J. Schmieg, D. W. Goodman, T. W. Root, S. B. Schwartz, and L. D. Schmidt, in Catalysis and automotive pollution control, (A. Crucq, A. Frennet, eds.) p. 215, Elsevier, Amsterdam 1987.
[19] T. Engel, G. Ertl, Adv. Catal. *28*, 2 (1979).
[20] S. H. Oh and J. E. Carpenter, J. Catal. *101*, 114 (1986).
[21] V. A. Drozdov, P. G. Tsyrul'nikov, V. V. Popovskii, J. D. Pankkarat'ev, A. A. Davydov, and E. M. Moroz, Kinet. Kat. *27* (3), 721 (1980).
[22] G. P. Gorelov and E. Kh. Kurumchin, Kinet. Kat. *27* (6), 1346 (1986).
[23] A. S. Sass, V. A. Shvets, G. A. Savel'eva, N. M. Popova, and V. B. Kazanskii, Kinet. Kat. *27* (4), 894 (1986).
[24] D. Beck, T. W. Capehart, and R. W. Hoffmann, Chem. Phys. Lett. *159* (2,3), 207 (1989).
[25] P. Lööt, B. Kasemo, and K. E. Keck, J. Catal. *118*, 339 (1989).
[26] E. L. Su, C. N. Montreuil, and W. G. Rothschild, Appl. Catal. *17*, 75 (1985).
[27] T. Jin, T. Okahara, G. J. Mains, and J. M. White, J. Phys. Chem. *91*, 3310 (1987).
[28] D. W. Daniel, J. Phys. Chem. *92*, 3891 (1988).
[29] J. T. Yates Jr., P. A. Thiel, and A. P. Merrill, J. Catal. *65*, 461 (1980).
[30] S. H. Oh, G. B. Fischer, J. E. Carpenter, and D. W. Goodmann, J. Catal. *100*, 360 (1986).
[31] E. Koberstein and G. Wannemacher, in: Catalysis and Automotive pollution control, (A. Crucq, A. Frennet, eds), p. 155, Elsevier 1987.
[32] W. R. C. Graham and D. T. Lynch, A.I.Ch.E. *33* (5), 792 (1987).
[33] D. T. Lynch, G. Emig, and S. E. Wanke, J. Catal. *97*, 456 (1986).
[34] C. T. Campbell and J. M. White, Appl. Surf. Sci, *1*, 347 (1978).
[35] R. Raval, G. Blyholder, S. Haq, and D. A. King, J. Phys. Coord. Mater *1*, SB 165 (1989).
[36] C. Li, Y. Sakata, T. Arai, K. Domen, K. Maruya, and T. Onishi, J. Chem. Soc. Faraday Trans. I, *85* (4), 929 (1989); *85* (6), 1451 (1989).
[37] J. Barrault and A. Alouche, Appl. Catal. *58*, 255 (1990).

Presented at the Discussion Meeting of the Deutsche Bunsen-Gesellschaft für Physikalische Chemie "In situ-Investigations of Physico-Chemical Processes at Interfaces" in Lahnstein from September 30th to October 2nd, 1992 E 8187